Available online at www.sciencedirect.com
SCIENCE DIRECT
Polymer 46 (2005) 11527–11539
polymer
www.elsevier.com/locate/polymer

Comprehensive analysis of stereoregularity and sequence distribution in 2-*N*-carbazolylethyl acrylate and methyl methacrylate copolymers by 2D NMR spectroscopy and their thermal studies

A.S. Brar*, Meghna Markanday

Department of Chemistry, Indian Institute of Technology, Delhi, New Delhi 110016, India

Received 19 May 2005; received in revised form 11 August 2005; accepted 3 September 2005
Available online 10 October 2005

Abstract

A series of 2-*N*-carbazolylethyl acrylate (C) and methyl methacrylate (M) copolymers with varying compositions were prepared in toluene at 60 °C using AIBN as an initiator. The molar outfeed ratio (F_C) for various compositions was determined from ^{1}H NMR spectra. Reactivity ratios calculated using Kelen–Tudos (KT) and non-linear error in variable (RREVM) methods were found to be $r_C = 0.43 \pm 0.8$ and $r_M = 2.78 \pm 0.52$. Molecular weight distribution was determined by gel permeation chromatography (GPC). The methine carbon of C unit showed splitting up to the pentad level in $^{13}C\{^1H\}$ NMR spectra and was found to be sensitive to the variation in C/M copolymer compositions. The backbone methylene and carbonyl carbons of both M and C unit along with α-methyl carbon of the M unit showed both compositional and configurational sensitivity. Distortionless enhancement by polarization transfer (DEPT) helped in differentiating the methylene carbon signals from the methine and methyl carbon resonances. 2D heteronuclear single quantum coherence (HSQC) and 2D total correlation spectroscopy (TOCSY) were used in tandem to deduce all spectral assignments. 2D heteronuclear multiple bond coherence (HMBC) played an important role in studying the stereoregularity of the carbonyl carbon. The trend in variation of glass transition temperature (T_g) of various C/M copolymer compositions was also studied.

Keywords: 2-*N*-carbazolylethyl acrylate; NMR; Microstructure

1. Introduction

Amorphous organic photosensitive polymer systems are new materials with potential application as recording media for holographic storage and real-time optical information processing [1,2]. Carbazole-based monomers have proved successful as the charge-transporting photoconductive component of the photorefractive (PR) polymers [3–13]. These polymers are widely used in industry because of their ease in modification and ready manufacturing. They have been tailored to obtain more robust and reliable PR materials exhibiting both photoconductive and electro-optic properties. 2-*N*-Carbazolylethyl acrylate/methyl methacrylate belongs to the class of photoconductive polymers [14–22] and has been used in photocopiers [23] and light-emitting diodes [24].

In view of their bulky pendant groups, these photoconductive polymers tend to possess a high glass transition temperature which makes their processing for making thin films difficult. It has been reported that copolymerization has a great influence on thermal properties of polymer [25,26].

The tacticity and conformation of polymer chain is very crucial in determining the transport properties especially, in case, of polymeric systems bearing pendant chromophores [27,28]. Hence, determination of microstructure of polymers is important for establishing correlation of charge-carrier transport property with tacticity. NMR has proven to be one of the most informative and revealing techniques for investigation of polymer microstructure [29–35].

Much work has been done to study the photoconductive properties of poly(2-*N*-carbazolylethyl acrylate) and the copolymers, but literature survey reveals that the microstructure of copolymers has not been reported in detail. Brar et al. has studied extensively the microstructure of various (meth) acrylate copolymer systems by various NMR techniques [36–38]. In this article, we report the microstructure of poly(2-*N*-carbazolylethyl acrylate-*co*-methyl methacrylate) using high-resolution 1D (^{1}H, $^{13}C\{^1H\}$, DEPT-135, 90, 45) and 2D (HSQC, TOCSY, HMBC) [35–43] NMR spectroscopy techniques. A comprehensive analysis of the complex

* Corresponding author. Tel.: +91 11 26591377; fax: +91 11 25195693.
E-mail address: asbrar@chemistry.iitd.ernet.in (A.S. Brar).

0032-3861/$ - see front matter © 2005 Elsevier Ltd. All rights reserved.
doi:10.1016/j.polymer.2005.09.006

and overlapped regions of $^{13}C\{^1H\}$ NMR spectra was done with the aid of various 2D NMR techniques. The variation in thermal stabilities and glass transition temperature (T_g) with varying copolymer compositions was also studied.

2. Experimental section

2.1. Materials

Carbazole (96%, Aldrich) was recrystallized from methanol. Ethylene carbonate (98%, Aldrich) and sodium hydride (50% oil dispersion, CDH) were used as supplied. Acryloyl chloride (98%, Aldrich) was distilled under reduced pressure and stored below 5 °C. Methyl methacrylate (M) (98%, Merck) was dried over CaH_2, vacuum distilled and kept below 5 °C before use. AIBN (Fluka) was recrystallized from methanol and stored at low temperature.

2.2. Monomer synthesis

The monomer 2-*N*-carbazolylethyl acrylate (C) was synthesized via a two-step reaction as reported elsewhere [28,44].

2.3. Polymerization

A series of 2-*N*-carbazolylethylacrylate/methyl methacrylate (C/M) copolymers with different molar infeed ratios were synthesized by solution polymerization using toluene as a solvent and AIBN as an initiator at 60 °C. The percentage conversion was measured gravimetrically and kept below 10% by precipitating the copolymers in methanol. They were further purified using $CHCl_3/CH_3OH$ as solvent and precipitant, respectively.

2.4. Characterization

All the 1D (^1H, $^{13}C\{^1H\}$, DEPT) and 2D (HSQC, TOCSY, HMBC) NMR spectra of the copolymers were recorded on Bruker DPX-300 spectrometer in $CDCl_3$ at frequencies of 300.1 and 75.5 MHz for ^1H and ^{13}C, respectively, at 25 °C using standard pulse sequences as reported earlier [45]. The signal intensities of the spectra peak were measured from the integrated areas calculated with electronic integrator. NMR measurements were made on 10% (w/v) polymer solutions.

The outfeed molar fraction (F_C) in the copolymers was determined experimentally from ^1H NMR spectra. The molecular weight (M_n) and the polydispersity index (M_w/M_n) were measured using gel permeation chromatography (GPC) equipped with a Waters 501 pump with guard column and a Waters 410 RI detector against polystyrene standards using THF as eluent at the flow rate of 0.3 ml/min at 30 °C. Differential scanning calorimetry (DSC) measurements were carried out on a Perkin–Elmer DSC-7 with a heating rate of 10 °C min^{-1}. Samples of 3–14 mg were sealed in aluminium pans and were submitted to repeated heating/cooling cycles. Thermogravimetry (TG) and differential thermal analysis (DTA) were carried out on Netzsch Simultaneous Thermoanalyse STA 409C apparatus under the following basic conditions: heating rate of 10 °C min^{-1}, sample weight of 5–18 mg, temperature interval from 50 to 800 °C.

3. Results and discussion

3.1. Copolymer composition and reactivity ratio determination

On the basis of relative areas of the proton resonances of $–OCH_2CH_2N–$ of C unit and $–OCH_3$ of M unit in the ^1H NMR spectra, F_C for various copolymer compositions was calculated as below:

$$F_C = \frac{I(OCH_2CH_2N)/4}{I(OCH_2CH_2N)/4 + I(OCH_3)/3}$$

Table 1 lists the F_C, molecular weight distribution and overall conversion of copolymers. The overall conversion to polymer was kept below 5% to avoid compositional drift. The theoretical F_C for various copolymers were determined as reported by Brar et al. [46]. The copolymer composition data was used to calculate the terminal model reactivity ratios by linear Kelen-Tudos method (KT) and nonlinear error-in-variables (RREVM) method, which were found to be $r_C = 0.43 \pm 0.08$, $r_M = 2.70 \pm 0.52$ and $r_C = 0.43$, $r_M = 2.78$, respectively.

3.2. ^1H NMR studies

The ^1H NMR spectrum of the C/M copolymer for $F_C = 0.47$ with the assignment of various resonance signals is shown in Fig. 1. The $–OCH_2CH_2N–$ protons of the C unit and the $–OCH_3$ protons of the M unit appear as a set of two separate signals centered around 3.56 and 4.31 ppm, respectively. The aromatic proton region extends from 6.68 to 8.13 ppm. The aliphatic proton region around 0.22–2.23 ppm is quite complex

Table 1
Theoretical and experimental F_C, molecular weight distribution, overall conversion and T_g of copolymers

Infeed molar fraction, f_C	Outfeed molar fraction		Conversion (wt%)	$M_w \times 10^{-4}$ (g/mol)	Polydispersity index (M_w/M_n)	T_g (°C)
	Experimental, F_C	Theoretical, F_C				
PC	–	–	–	0.745	1.5	80
0.9	0.79	0.79	2.9	0.964	1.6	85
0.7	0.47	0.48	3.2	1.204	1.3	90
0.6	0.38	0.37	3.5	1.468	1.5	108
0.5	0.27	0.27	4.4	1.645	1.4	112

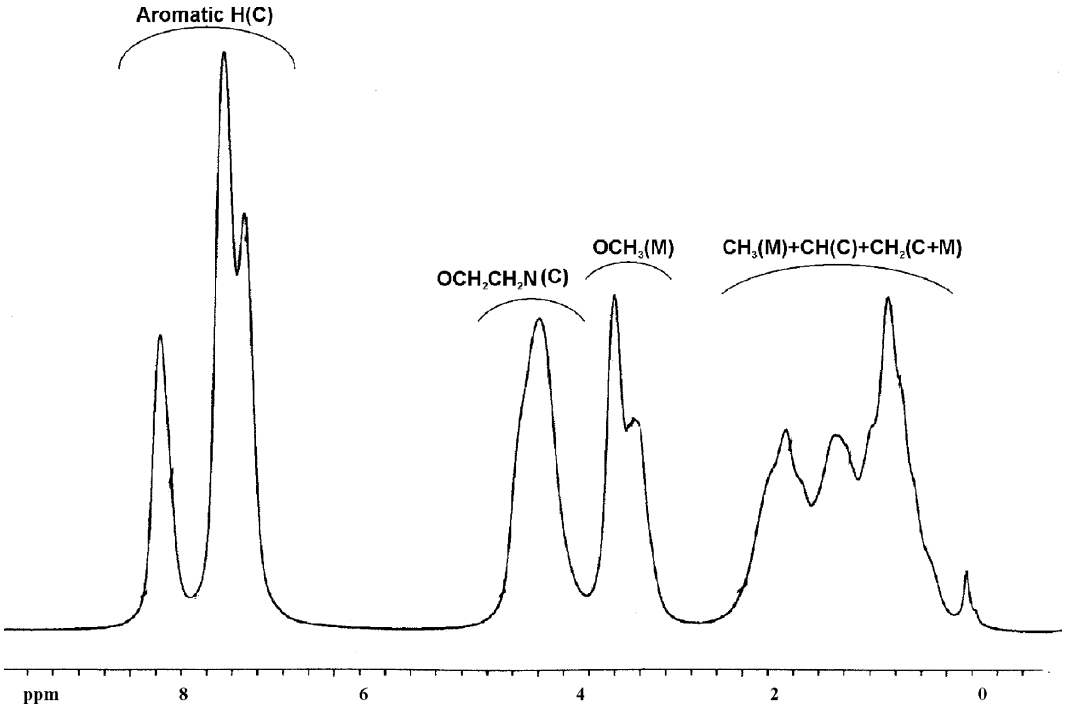

Fig. 1. ^{1}H NMR spectrum of C/M copolymer for $F_C = 0.48$ in $CDCl_3$ at 25 °C.

and overlapped and can be tentatively assigned to the α-methyl carbon of M unit, methine carbon of C unit and methylene carbons of M and C units. 1D (DEPT, $^{13}C\{^{1}H\}$) and 2D (HSQC, HMBC, TOCSY) NMR techniques were utilized hand in hand in order to resolve the overlapped signals and completely assign the ^{1}H NMR spectrum.

3.3. $^{13}C\{^{1}H\}$ NMR studies

The $^{13}C\{^{1}H\}$ NMR spectrum of the C/M copolymer ($F_C = 0.48$) is shown in Fig. 2. The α-methyl carbon resonance of the M unit appears around 15.89–22.45 ppm, while the carbonyl carbon of both the M and C units can be assigned to the region 173.48–178.68 ppm. The appearance of these carbon resonances as complex and overlapped indicates their sensitivity towards various compositional and configurational sequences. The side chain $-OCH_2$ and $-NCH_2$ methylene carbons of C unit along with $-OCH_3$ carbon of the M unit appear as singlet around 62.07, 42.05 and 51.75 ppm, respectively, reflecting their insensitivity to compositional and configurational sequences. The aromatic carbons of the side-chain carbazole moiety appear as singlet in the region 108.62–140.23 ppm as reported by Dias et al. [47,48].

The spectral region around 33.87–55.21 ppm is quite complex and overlapped and can be assigned to the aliphatic carbons of the C and M units. Utilizing the DEPT-135 (Fig. 2) spectrum in conjunction with $^{13}C\{^{1}H\}$ NMR spectrum, this highly complex region can be resolved as in DEPT-135 the methylene carbon signal appears as a negative phase while the methine and methyl carbon signals appear in the positive phase. The resonance signals around 33.87–36.23 and 42.34–55.21 ppm can be assigned to backbone methylene carbons of the C and M units, respectively. From DEPT-90 spectrum the methine carbon of the C unit can be assigned to region around 36.44–41.68 ppm. The quaternary carbon of M unit has been assigned to 43.01–45.82 ppm.

3.4. Analysis of α-methyl region

The α-methyl carbon of the M unit resonates from 16.01 to 22.33 ppm in the $^{13}C\{^{1}H\}$ NMR spectrum. Fig. 3 shows the variation in the resonance signals of the α-methyl carbon (M) unit in various copolymer compositions in comparison with the homopolymer, PMMA [43]. The α-methyl region in PMMA has been assigned to the mm (21.07 ppm), mr (18.76 ppm) and rr (16.49 ppm) of MMM triad sequence, respectively.

On speculating the changes in the intensities of the resonance peaks with increase in the M content in the copolymers, α-methyl region of C/M copolymers can be assigned to various configurational sensitive triad sequences. The region 16.01–22.33 ppm can be divided into five regions viz. (I) 16.01–17.35 ppm, (II) 17.35–18.78 ppm, (III) 18.78–19.57 ppm, (IV) 19.57–21.01 ppm and (V) 21.01–22.33 ppm which can be assigned to rr-MMM, r(MMC + CMM), (rm + mr)MMM, CMC and mm-MMM triads, respectively.

A step-by-step approach has been adopted in comprehensively speculating and then, confirming the various assignments using 2D HSQC NMR spectrum.

3.4.1. Region I (16.01–17.35 ppm) and region II (17.35–18.78 ppm)

The resonance peaks show further splitting up to the pentad level which can be assigned to various M-centered pentads by observing the change in intensity with increase in M content of

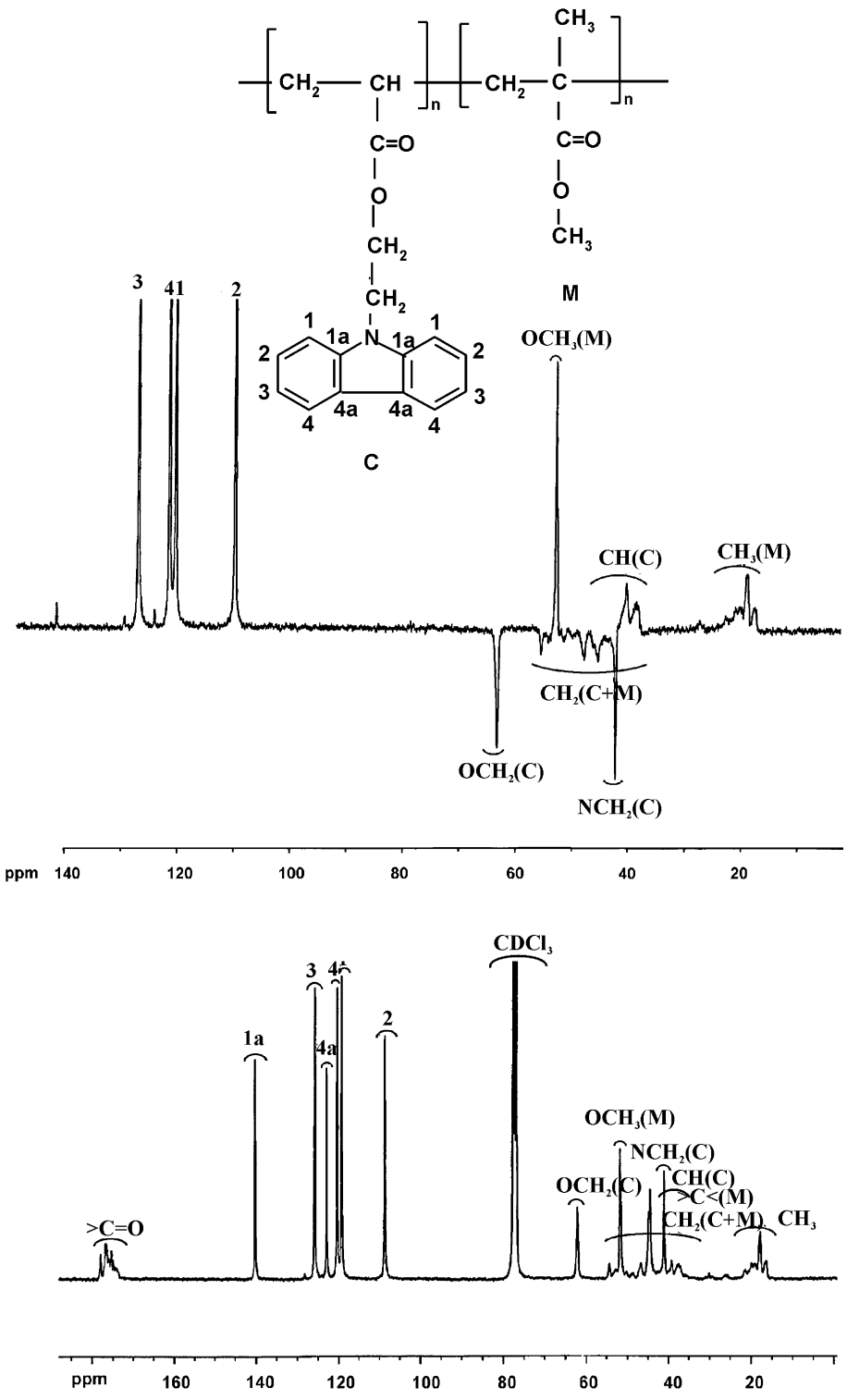

Fig. 2. (a) $^{13}C\{^{1}H\}$ NMR spectrum and (b) DEPT-135 NMR spectrum of C/M copolymer with $F_C = 0.48$ in $CDCl_3$ at 25 °C.

the C/M copolymers. Fig. 4 shows the 2D HSQC spectrum of α-methyl region for three different compositions. The cross-peak at 16.81/0.85 ppm (1) can be assigned to MrMrM triad while the cross-peaks centered at 18.24/0.74 ppm (2) and 18.47/0.85 ppm (3) can be assigned to MMrMrCM and CMrMrCC, respectively.

3.4.2. Region III (18.78–19.57 ppm)

MmMrM triad region splits further up to the pentad level and thereby, show cross-peaks centered at 18.91/1.05 ppm (4), 19.17/0.69 ppm (5) and 19.39/0.75 ppm (6) which have been assigned to MMmMrMM, MMmMrMC and CMmMrMC, respectively.

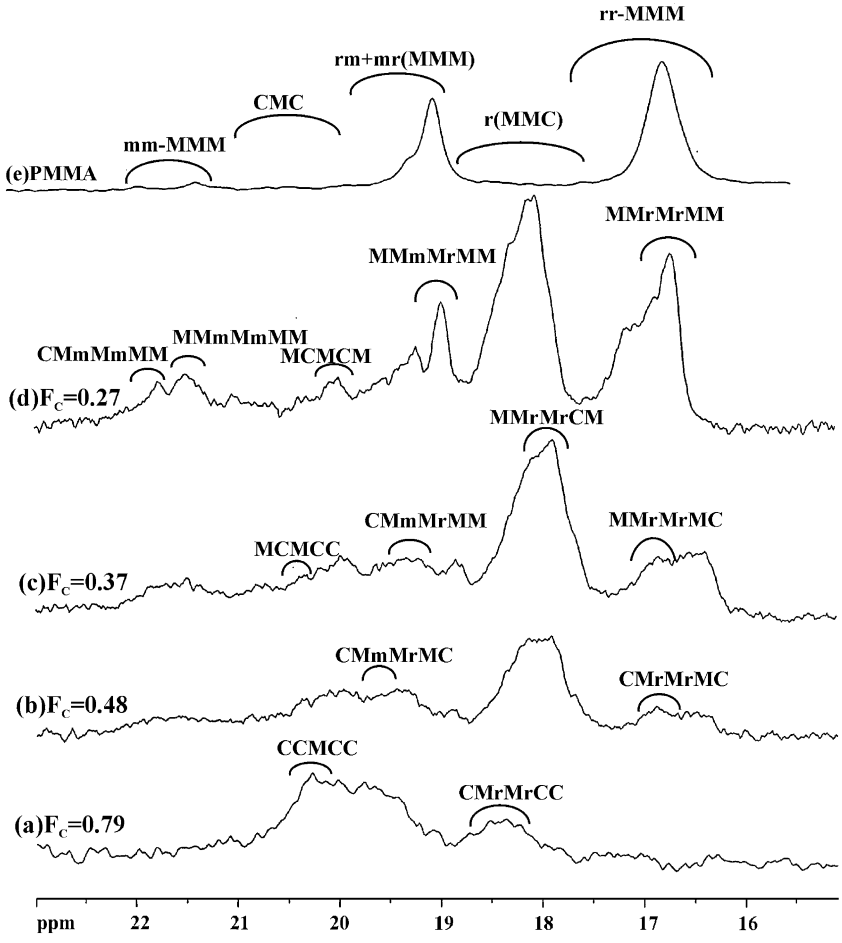

Fig. 3. Expanded α-methyl carbon resonance patterns of PMMA and C/M copolymer with increasing F_M in $CDCl_3$ at 25 °C.

3.4.3. Region IV (19.57–21.01 ppm) and region V (21.01–22.33 ppm)

The CMC triad further splits into pentads and show cross-peaks centered at 19.69/0.55 ppm (7), 19.98/0.81ppm (8) and 20.25/0.41 ppm (9) which can be assigned to MCMCM, CCMCM and CCMCC, respectively. The cross-peaks around 21.46/0.63 ppm (10) and 21.53/0.98 ppm (11) have been assigned to MMmMmMM and MMmMmMC pentads, respectively. Table 2 gives the peak positions of spectral assignments based on the $^{13}C\{^1H\}$ NMR and 2D HSQC spectra.

Table 3 compares the M-centered triad fractions with theoretical values that were calculated from reactivity ratios [46]. The experimentally observed M-centered triad fractions were estimated by determining the area under the resonance peaks using Lorentzian curve-fitting. Curve-fitting was done by an electronic integrator. Good agreement is seen between the theoretical and experimental triad fractions thereby, supporting the assignments.

3.5. Analysis of methine region

Fig. 5 shows the comparison of DEPT-90 NMR spectra of methine carbon region of C/M copolymers for different copolymer compositions with that of the homopolymer, poly(2-*N*-carbazolylethyl acrylate) (PC). Increasing C content in the copolymer influences the intensity of various signals differently. On this basis, the methine carbon signals from 36.44 to 41.68 ppm can be divided into three regions viz. MCM triad region from 36.44 to 38.73 ppm, MCC triad region from 38.73 to 40.43 ppm and CCC triad region from 40.43 to 41.68 ppm. All the triads are C-centered as the methine carbon signal is observed due to the C unit of the C/M copolymers and show only compositional sensitivity.

Further, each region can be seen splitted up to pentad level which can be only tentatively assigned on the basis of $^{13}C\{^1H\}$ NMR. Thus, cross-peaks observed in 2D HSQC NMR spectrum are investigated to make unambiguous assignments. Fig. 6 shows the 2D HSQC spectrum of the methine region of C/M copolymers for three different compositions.

MCM triad shows three cross-peaks in 2D HSQC NMR spectrum (Fig. 6(c)) centered at 37.18/2.13 ppm (12), 37.68/2.01 ppm (13) and 38.21/2.20 ppm (14) which can be unequivocally assigned to the three pentads MMCMM (12), MMCMC (13) and CMCMC (14), respectively. Similarly, MCC triad shows three cross-peaks in 2D HSQC NMR spectrum (Fig. 6(a) and (c)) at 39.23/2.12 ppm (15), 39.49/2.01 ppm (16) and 39.71/2.06 ppm (17) which can be assigned

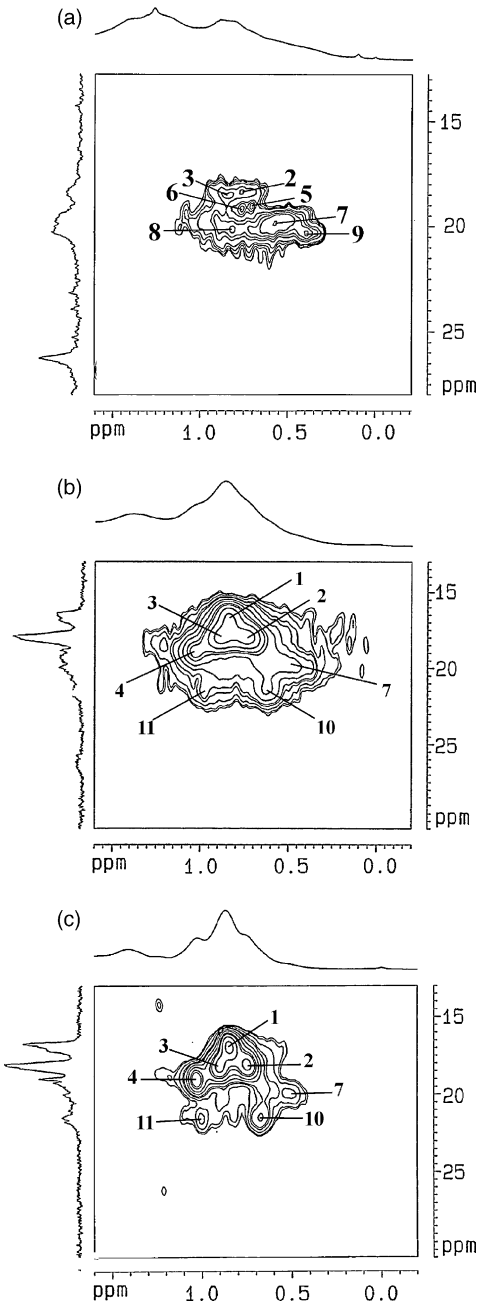

Fig. 4. 2D HSQC NMR spectra of C/M copolymers showing α-methyl region in $CDCl_3$ at 25 °C. (a) $F_C=0.79$ (b) $F_C=0.48$ and (c) $F_C=0.27$.

to MMCCM, MMCCC and CMCCC, respectively. CCC triad shows only one cross-peak in 2D HSQC NMR spectrum (Fig. 6(a) and (b)) at 40.89/1.98 ppm (18) and can be assigned to CCCCC pentad. It is evident from the 2D HSQC NMR spectrum that the methine proton lays in a narrow range of 1.98–2.13 ppm in the ^{1}H NMR spectra.

This information helps in analyzing the geminal couplings between methine protons of C unit in CC and CM centered dyads with the methylene protons of both C and M units in the C/M copolymers in the 2D TOCSY NMR spectra (Fig. 7(a)). Three cross-correlation peaks, 1.49/2.10 ppm (K), 1.21/2.10 ppm (L) and 1.01/2.10 ppm (J) can be assigned to the

Table 2
Spectral assignments of α-methyl carbon resonances in $^{13}C\{^1H\}$ NMR and 2D HSQC spectra

Peak	Peak assignments	Peak position ($^{13}C\{^1H\}$ NMR; ppm)	Peak position (2D HSQC; $^{13}C/^1H$; ppm)
1	MrMrM	16.72	16.81/0.85
2	CMrMrCM	18.13	18.24/0.74
3	CMrMrCC	18.41	18.47/0.85
4	MMmMrMM	18.94	18.91/1.05
5	MMmMrMC	19.14	19.17/0.69
6	CMmMrMC	19.41	19.39/0.75
7	MCMCM	20.02	19.69/0.55
8	CCMCM	20.20	19.98/0.81
9	CCMCC	20.31	20.25/0.41
10	MMmMmMM	21.49	21.46/0.63
11	MMmMmMC	21.62	21.53/0.98

Table 3
M-centered triad fractions determined from the α-methyl carbon resonance patterns

F_M	Triad fractions					
	Observed			Calculated		
	MMM	MMC + CMM	CMC	MMM	MMC + CMM	CMC
0.21	0.04	0.32	0.64	0.06	0.36	0.58
0.52	0.24	0.52	0.24	0.30	0.50	0.21
0.63	0.37	0.47	0.16	0.42	0.46	0.12
0.73	0.52	0.40	0.08	0.54	0.39	0.07

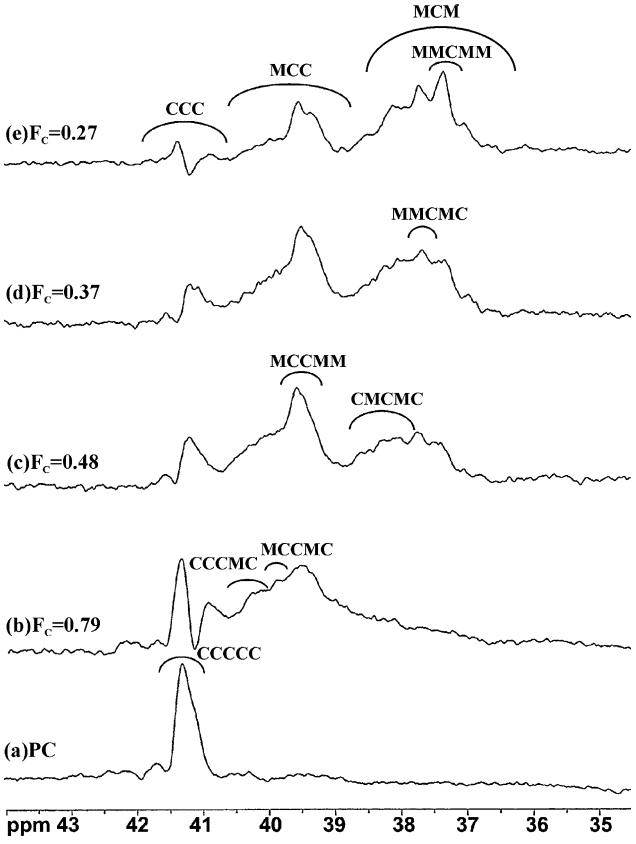

Fig. 5. DEPT-90 NMR spectra showing the methine carbon resonance patterns of PC and C/M copolymers with decreasing F_C in $CDCl_3$ at 25 °C.

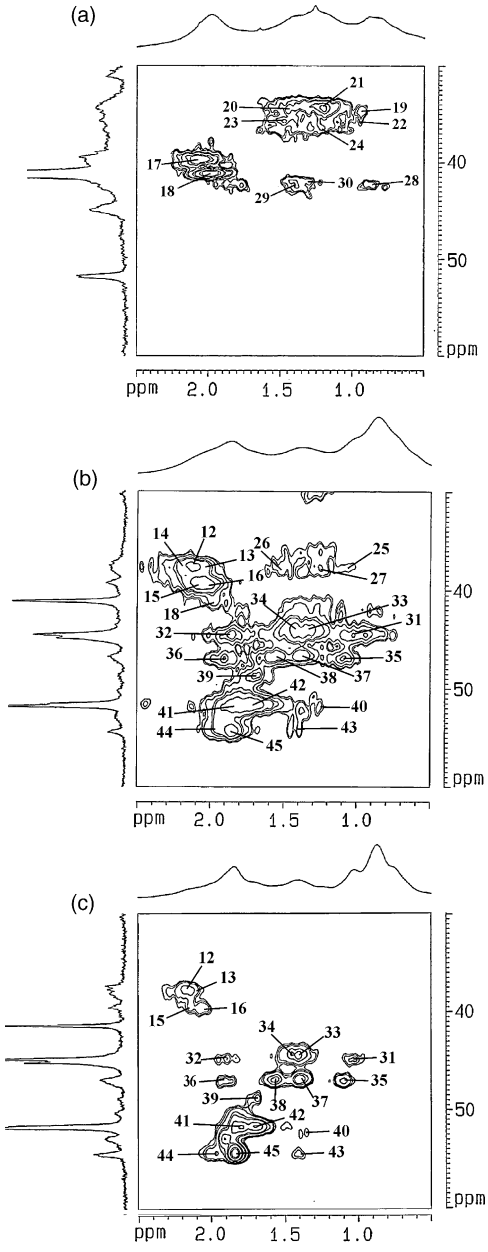

Fig. 6. 2D HSQC NMR spectra of C/M copolymers showing the methine and backbone methylene region in $CDCl_3$ at 25 °C. (a) $F_C=0.79$ (b) $F_C=0.48$ and (c) $F_C=0.27$.

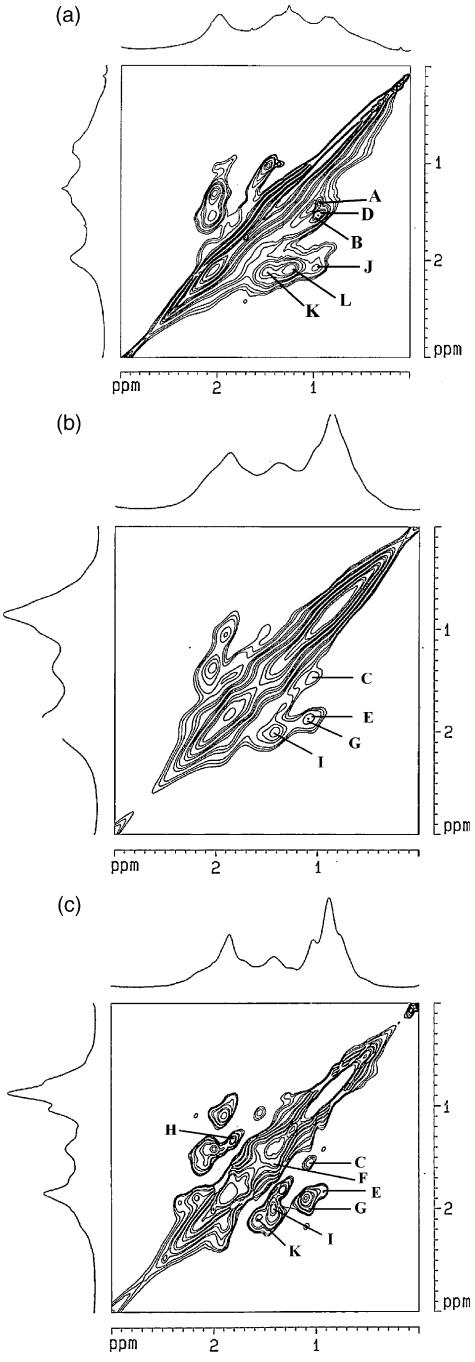

Fig. 7. 2D TOCSY NMR spectra of C/M copolymers in $CDCl_3$ at 25 °C (a) $F_C=0.79$ (b) $F_C=0.48$ and (c) $F_C=0.27$.

geminal between methine proton of CC and CM unit with the backbone methylene proton of CmC/CmM (Hb), CrC/CrM (Hc) and CmC/CmM (Ha), respectively. Table 4 gives the spectral assignments for methine region on the basis of $^{13}C\{^1H\}$ NMR and 2D HSQC.

Table 5 enlists the observed and calculated values of C-centered triad fractions. The experimentally observed C-centered triad fractions were estimated by determining the area under the resonance peaks using Lorentzian curve-fitting. Curve-fitting was done by an electronic integrator. The comparison shows generally good agreement between experimental area and calculated C-centered triad fractions.

Table 4
Spectral assignments of methine carbon resonance $^{13}C\{^1H\}$ NMR and 2D HSQC spectra

Peak	Peak assignments	Peak position ($^{13}C\{^1H\}$ NMR; ppm)	Peak position (2D HSQC; $^{13}C/^1H$; ppm)
12	MMCMM	37.35	37.18/2.13
13	MMCMC	37.72	37.68/2.01
14	CMCMC	38.19	38.21/2.20
15	MCCMM	39.27	39.23/2.12
16	MCCMC	39.45	39.49/2.01
17	CCCMC	39.82	39.71/2.06
18	CCCCC	39.91	40.89/1.98

Table 5
C-centered triad fractions determined from methine carbon resonance patterns

F_C	Triad fractions					
	Observed			Calculated		
	CCC	CCM + MCC	MCM	CCC	CCM + MCC	MCM
0.79	0.68	0.29	0.03	0.63	0.33	0.04
0.48	0.27	0.50	0.23	0.25	0.50	0.25
0.37	0.13	0.52	0.35	0.15	0.48	0.37
0.27	0.10	0.44	0.46	0.09	0.42	0.49

3.6. Analysis of backbone methylene region

The backbone methylene region lies between 33.87 and 55.21 ppm in $^{13}C\{^1H\}$ NMR spectrum. Fig. 8 shows the comparison of this region for various C/M copolymer compositions with the respective homopolymers. The stretch of signals from 33.87 to 55.21 ppm can be trifurcated into region I (33.87–40.01 ppm), region II (40.01–47.55 ppm) and region III (47.55–55.21 ppm) assigned to CC, CM and MM dyads, respectively, which can be seen splitting further into tetrads. On speculating the trend of variation in intensity of resonance signals with increase/decrease of C content these tetrads can be tentatively assigned in $^{13}C\{^1H\}$ NMR spectrum.

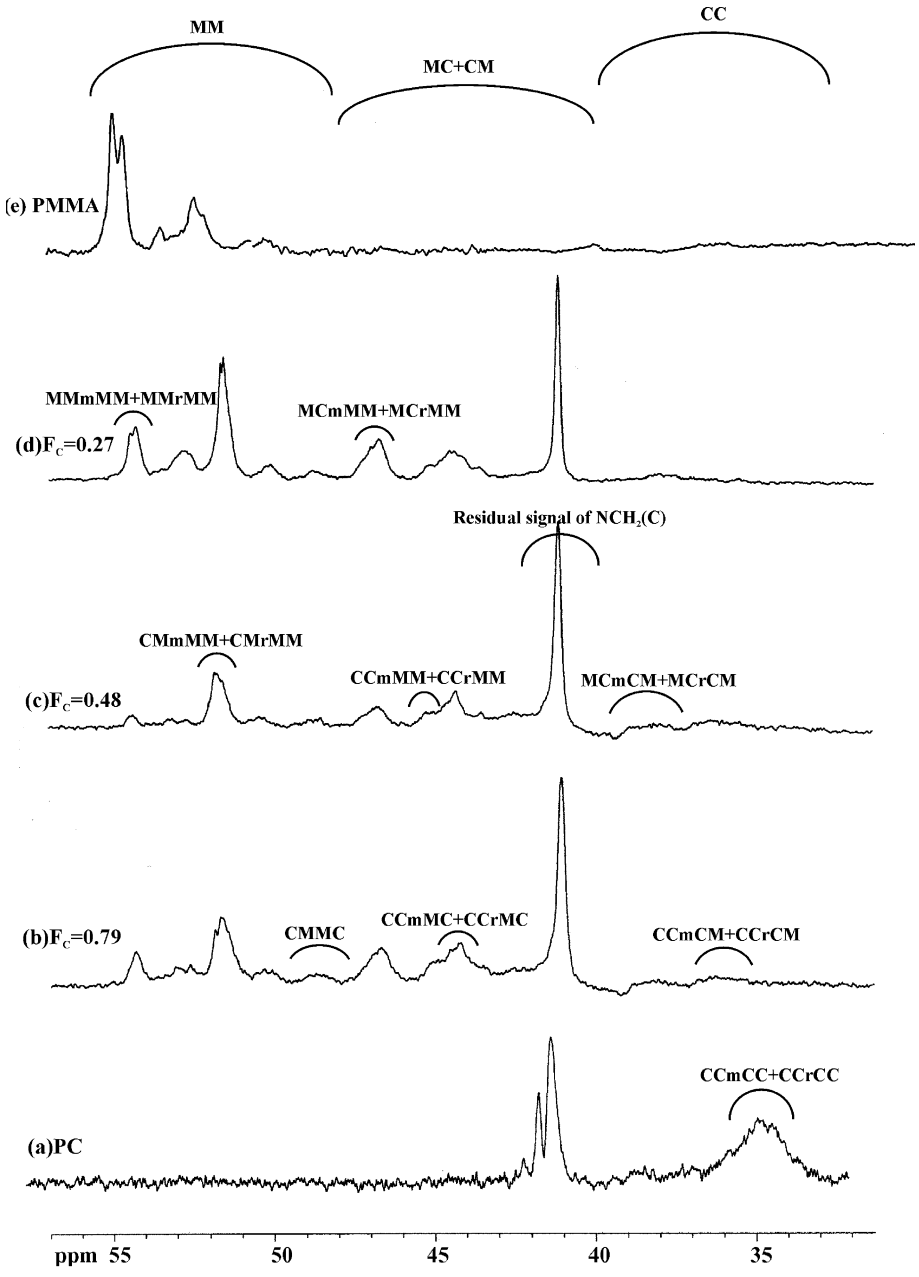

Fig. 8. Expanded backbone methylene carbon resonance patterns of PMMA, PC and C/M copolymers with decreasing F_C in $CDCl_3$ at 25 °C.

To make unequivocal assignments 2D HSQC NMR spectra in conjunction with 2D TOCSY NMR spectra are utilized.

3.6.1. Region I (33.87–40.01 ppm), CC dyad

This region further splits into tetrads. The cross-peaks centered at 34.89/0.95 ppm (19) and 34.89/1.43 ppm (20) in 2D HSQC NMR spectrum (Fig. 6(a)) have been assigned to the tetrad CCmCC corresponding to the non-equivalent protons CCmCC (Ha) and CCmCC (Hb). A single cross-correlation peak centered at 0.95/1.43 ppm (A) is observed due to geminal coupling between these protons in 2D TOCSY NMR spectra (Fig. 7(a)). CCrCC tetrad appears as a single cross-peak that lies between the two cross-peaks 19 and 20 at 34.89/1.19 ppm (21).

Similarly, the tetrad CCmCM shows two cross-peaks in 2D HSQC NMR (Fig. 6(a)) at 36.38/0.94 ppm (22) and 36.38/1.48 ppm (23) corresponding to the non-equivalent meso protons CCmCM (Ha) and CCmCM (Hb), respectively. These two protons show a single cross-peak at 0.94/1.48 ppm (B) in 2D TOCSY NMR spectra as shown in Fig. 8(a). CCrCM tetrad is seen as a single cross-peak lying in between 22 and 23 at 36.38/1.21 ppm (24).

As the content of M unit increases in the C/M copolymers, the cross-peaks due to tetrad MCCM can be observed only at higher F_M. In Fig. 6(b) two cross-peaks centered at 38.15/1.10 ppm (25) and 38.15/1.50 ppm (26) in 2D HSQC NMR can be assigned to the two non-equivalent meso protons corresponding to MCmCM (Ha) and MCmCM (Hb), respectively. A cross-peak at 1.11/1.50 ppm (C) due to coupling between these protons is seen in 2D TOCSY NMR spectra in Fig. 7(b) and 7c. MCrCM tetrad appears as a single cross-peak in between 25 and 26 at 38.15/1.28 ppm (27) in 2D HSQC NMR spectra.

In general, due to the bulky pendant carbazole containing side-group the contours are not very distinct and appear extended and distorted.

3.6.2. Region II (40.01–47.55 ppm), CM dyad

The racemic protons of methylene carbon are equivalent in case of the CC/MM dyad but they experience different chemical environments in case of the CM dyad. Thus, they appear as two distinct peaks in 2D HSQC NMR spectra and give a single cross-peak in 2D TOCSY NMR spectra.

In Fig. 6(a), CCmMC tetrad appears as two cross-peaks at 42.48/0.94 ppm (28) and 42.48/1.46 ppm (29) corresponding to CCmMC (Ha) and CCmMC (Hb), respectively. They give a single cross-peak at 0.94/1.46 ppm (D) in 2D TOCSY NMR spectra (Fig. 7(a)). The CCrMC appears as a single cross-peak in between 28 and 29 at 42.48/1.31 ppm (30).

CCmMM tetrad also shows two cross-peaks at 44.47/1.05 ppm (31) and 44.47/1.88 ppm (32) in the 2D HSQC NMR corresponding to the CCmMM (Ha) and CCmMM (Hb), respectively (Fig. 6(b) and (c)). A single cross-peak occurs at 1.05/1.88 ppm (E) in 2D TOCSY NMR spectra due to coupling between them (Fig. 7(b) and (c)). In CCrMM the non-equivalent racemic protons also give two cross-peaks in 2D HSQC NMR spectra at 44.47/1.36 ppm (33) and 44.47/1.46 ppm (34) corresponding to CCrMM (Hc) and CCrMM (Hd) protons, respectively as shown in Fig. 6(b) and (c). The coupling of these two protons results in a cross-peak in the 2D TOCSY NMR spectra at 1.36/1.46 ppm (F) (Fig. 7(c)).

In Fig. 6(c) MCmMM tetrad shows two cross-peaks at 46.85/1.12 ppm (35) and 46.85/1.89 ppm (36) in the 2D HSQC NMR spectra corresponding to MCmMM (Ha) and MCmMM (Hb), respectively. A single cross-peak appears in 2D TOCSY NMR spectra at 1.12/1.89 ppm (G) as shown in Fig. 7(b) and (c). The MCrMM tetrad gives two cross-peaks at 46.85/1.38 ppm (37) and 46.85/1.58 ppm (38) in the 2D HSQC NMR spectra corresponding to MCrMM (Hc) and MCrMM (Hd).

3.6.3. Region III (47.55–55.21 ppm), MM dyad

CMMC tetrad gives a single cross-peak in the 2D HSQC NMR spectra at 48.87/1.68 ppm (39), while the CMmMM tetrad gives two cross-peaks at 52.01/1.35 ppm (40) and 52.01/1.83 ppm (41) corresponding to CMmMM (Ha) and CMmMM (Hb) (Fig. 6(b) and (c)). CMrMM tetrad gives a cross-peak lying in between 40 and 41 at 52.01/1.69 ppm (42). A cross-correlation peak at 1.96/1.35 ppm (H) in 2D TOCSY NMR spectra (Fig. 7(b)) corresponds to the coupling of non-equivalent meso protons of CMmMM tetrad. Similarly, MMmMM shows two cross-peaks at 54.57/1.39 ppm (43) and 54.57/1.96 ppm (44) corresponding to MMmMM (Ha) and MMmMM (Hb). The two protons couple and thus, show a peak at 1.39/1.96 ppm (I) in 2D TOCSY NMR spectra.

Table 6
Spectral assignments of backbone methylene carbon resonance in 2D HSQC spectra

Peak	Peak assignments	Peak position (2D HSQC; $^{13}C/^{1}H$; ppm)
19	CCmCC (Ha)	34.89/0.95
20	CCmCC (Ha)	34.89/1.43
21	CCrCC	34.89/1.19
22	CCmCM (Ha)	36.38/0.94
23	CCmCM (Hb)	36.38/1.48
24	CCrCM	36.38/1.21
25	MCmCM (Ha)	38.15/1.10
26	MCmCM (Hb)	38.15/1.50
27	MCrCM	38.15/1.28
28	CCmMC (Ha)	42.48/0.94
29	CCmMC (Hb)	42.48/1.46
30	CCrMC	42.48/1.31
31	CCmMM (Ha)	44.47/1.05
32	CCmMM (Hb)	44.47/1.88
33	CCrMM (Hc)	44.47/1.36
34	CCrMM (Hb)	44.47/1.46
35	MCmMM (Ha)	46.85/1.12
36	MCmMM (Hb)	46.85/1.89
37	MCrMM (Hc)	46.85/1.38
38	MCrMM (Hd)	46.85/1.58
39	CMMC	48.87/1.68
40	CMmMM (Ha)	52.01/1.35
41	CMmMM (Hb)	52.01/1.83
42	CMrMM	52.01/1.69
43	MMmMM (Ha)	54.57/1.39
44	MMmMM (Hb)	54.57/1.96
45	MMrMM	54.57/1.82

Table 7
Cross-correlation peak assignments in 2D TOCSY spectra for coupling between geminal and vicinal protons of C/M copolymers

Peak	Coupled protons		Cross-correlation peak position ($^1H/^1H$; ppm)
	Proton I	Proton II	
A	CH_2 of CCmCC (Ha)	CH_2 of CCmCC (Hb)	0.95/1.43
B	CH_2 of CCmCM (Ha)	CH_2 of CCmCM (Hb)	0.94/1.48
C	CH_2 of MCmCM (Ha)	CH_2 of MCmCM (Hb)	1.11/1.50
D	CH_2 of CCmMC (Ha)	CH_2 of CCmMC (Hb)	0.94/1.46
E	CH_2 of CCmMM (Ha)	CH_2 of CCmMM (Hb)	1.05/1.88
F	CH_2 of CCrMM (Hc)	CH_2 of CCrMM (Hd)	1.36/1.46
G	CH_2 of MCmMM (Ha)	CH_2 of MCmMM (Hb)	1.12/1.89
H	CH_2 of CMmMM (Ha)	CH_2 of CMmMM (Hb)	1.35/1.83
I	CH_2 of MMmMM (Ha)	CH_2 of MMmMM (Hb)	1.39/1.96
J	CH of CCC	CH_2 of CmC (Ha)	1.01/2.10
K	CH of CCC	CH_2 of CmC (Hb)	1.49/2.10
L	CH of CCC	CH_2 of CrC (Hc)	1.21/2.10

Table 8
Comparison of experimental and calculated dyad distributions determined from methylene carbon resonance patterns

F_C	Dyad distributions					
	Observed			Calculated		
	CC	CM	MM	CC	CM	MM
0.79	0.68	0.30	0.02	0.63	0.32	0.05
0.48	0.30	0.46	0.24	0.24	0.48	0.28
0.37	0.19	0.42	0.39	0.14	0.44	0.41
0.27	0.13	0.36	0.51	0.08	0.38	0.53

Table 9
Spectral assignments of carbonyl carbon resonance in 2D HMBC spectra

Peak	Coupled carbonyl carbon with various protons		Peak position (2D HMBC; $^{13}C/^1H$; ppm)
	Carbon	Proton	
46	CO of MrMrM	α-methyl of MrMrM	178.21/0.83
47	CO of MmMrM	α-methyl of CMmMrMC	177.12/0.74
48	CO of MmMrM	α-methyl of MMmMrMM	177.01/1.03
49	CO of MmMrM	α-methyl of MMmMrMC	176.79/0.71
50	CO of MmMmM	α-methyl of MmMmM	176.79/0.67
51	CO of MmMmM	α-methyl of MmMmM	176.75/0.62
52	CO of CMC	α-methyl of MCMCM	176.31/0.55
53	CO of CMC	α-methyl of MCMCC	175.59/0.79
54	CO of MMmM	CH_2 of MMmMM	178.43/1.91
55	CO of MMmM	CH_2 of CMmMM (Ha)	178.43/1.82
56	CO of MMmM	CH_2 of CMmMM (Hb)	177.59/1.35
57	CO of MMmM	CH_2 of MMmMM	177.23/1.38
58	CO of CMC	CH_2 of CCmMC	176.39/0.95

The MMrMM tetrad appears as a cross-peak in between 43 and 44 at 54.57/1.82 ppm (45). Tables 6 and 7 gives the spectral assignments of backbone methylene carbon based on 2D HSQC and 2D TOCSY spectra respectively.

Table 8 compared observed resonance areas with dyad probabilities calculated for copolymers from monomer feed compositions and monomer reactivity ratios of $r_C=0.43$ and $r_M=2.78$.

3.7. Analysis of the carbonyl region

Both monomer contain carbonyl carbon which show highly complex and overlapped signals in $^{13}C\{^1H\}$ NMR spectra (Fig. 10). We resort to 2D HMBC studies for investigating the compositional and configurational sensitivity of the carbonyl

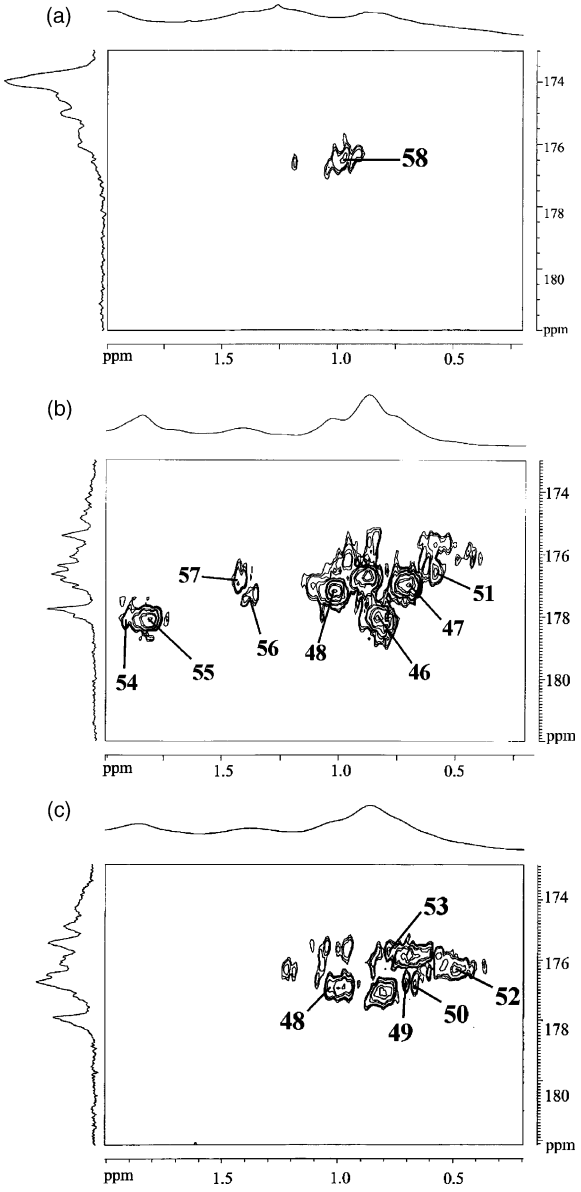

Fig. 9. 2D HMBC NMR spectra of C/M copolymers in $CDCl_3$ at 25 °C. (a) $F_C=0.79$ (b) $F_C=0.48$ and (c) $F_C=0.27$.

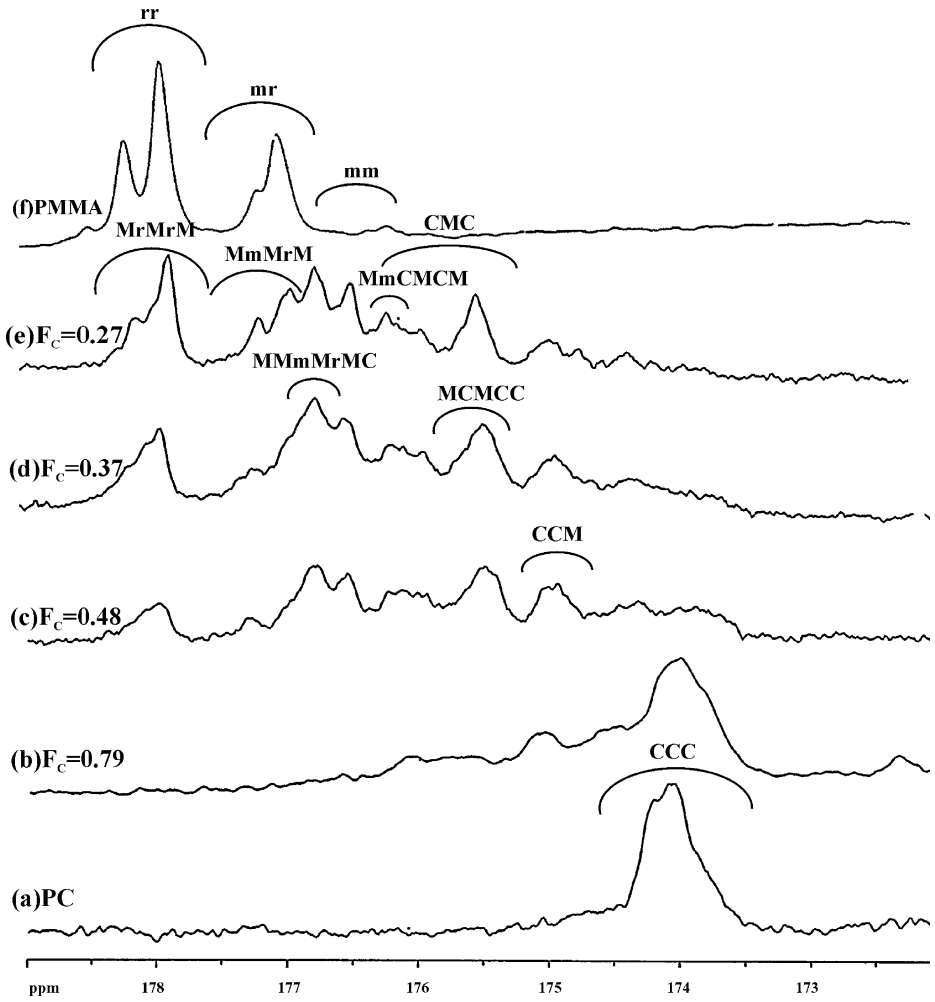

Fig. 10. Expanded carbonyl carbon region of PMMA, PC and C/M copolymers with decreasing F_C in $CDCl_3$ at 25 °C.

carbon, wherein we can see 1,3-bond order couplings of carbonyl carbon with α-methyl and backbone methylene protons.

Considering the coupling of carbonyl carbon with α-methyl protons only, M-centered triads will be observed. Cross-peaks (46) at 178.21/0.83 ppm appear due to coupling of carbonyl carbon of MrMrM triad with the α-methyl proton of MrMrM triad. Cross-peaks 177.12/0.74 ppm (47), 177.01/1.03 ppm (48) and 176.79/0.71 ppm (49) correspond to coupling of carbonyl carbon of MmMrM triad with α-methyl protons of CMmMrMC, MMmMrMM and MMmMrMC pentads, respectively. The coupling of carbonyl carbon and α-methyl protons of MmMmM triad results in cross-peaks 176.79/0.67 ppm (50) and 176.75/0.62 ppm (51) as shown in Fig. 9(b) and (c).

The coupling of carbonyl carbon of CMC triad with α-methyl protons of MCMCM and MCMCC pentads give cross-peaks at 176.31/0.55 ppm (52) and 175.59/0.79 ppm (53), respectively (Fig. 10).

The coupling of carbonyl carbon with backbone methylene protons can also be seen where MmM dyad shows cross-peaks at 54, 55, 56 and 57 corresponding to its coupling with MMmMM, CMmMM (Ha), CMmMM (Hb) and MMmMM tetrads, respectively.

The cross-peak 58 at 176.39/0.95 ppm (Fig. 9(a)) appears due to coupling of carbonyl carbon of CMC triad with β-methylene protons of CCmMC tetrad.

On the basis of these assignments the labeled 2D HMBC spectra for the three different compositions are shown in Fig. 9.

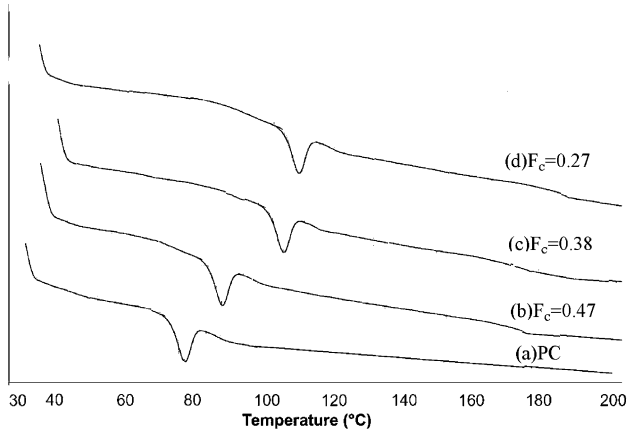

Fig. 11. DSC curves of (a) PC (b) F_C=0.48 (c) F_C=0.38 and (d) F_C=0.27.

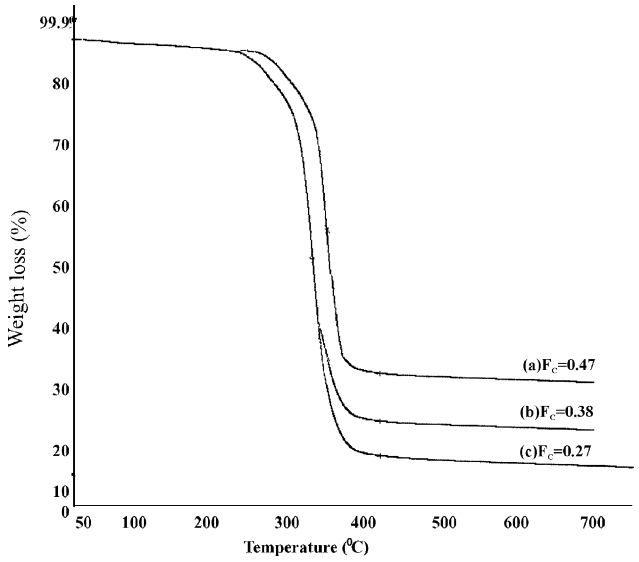

Fig. 12. TGA curves of (a) $F_C=0.48$ (b) $F_C=0.38$ and (c) $F_C=0.27$.

Table 9 gives the spectral assignments of carbonyl carbon based on 2D HMBC studies.

3.8. Thermal studies

The glass transition temperatures (T_g) [49,50] of these polymers were determined by DSC. The DSC curves are shown in Fig. 11. The T_g value of homopolymer, PC was obtained as 80 °C. The T_g values of copolymers lay between 80 and 112 °C depending on an increase in M content (Table 1). All the polymer samples are amorphous and show only a single glass transition temperature. Comparing the T_g of these polymers with that of PVK ($T_g=500$ K) wherein the carbazole moiety is directly attached to the backbone chain, we observe a major decline. The conformational stiffness of the carbazole group results in a higher T_g. Thus, introduction of flexible spacers between main-chain and carbazole ring renders flexibility and prevents tight packing between polymeric main-chains. This results in an increase of free volume in the homopolymer, PC leading to a lower T_g. It is advantageous to obtain polymers with low T_g as it would facilitate the chromophore to reorient and take advantage of the orientation enhancement effect, which is beneficial to the PR effect [51].

Experimentally, an increase in the T_g with increase in the M content of C/M copolymers is observed. This observation can be explained by the fact that the T_g of the copolymer is influenced by the respective homopolymers and thus, as T_g of respective homopolymers PC and PMMA in this case is 80 and 100 °C, respectively, the resulting copolymers have their T_g in the range of 80–100 °C.

The thermal stability of polymers was characterized by TGA. Representative TGA curves are shown in Fig. 12. It can be observed that all polymers start to lose weight around 220 °C. With a decrease in C content of C/M copolymers, the rigidity also decreases thereby exhibiting lower thermal stability than the corresponding homopolymer.

4. Conclusions

The value of reactivity ratios obtained using KT and EVM methods are $r_C=0.43\pm0.08$, $r_M=2.70\pm0.52$ and $r_C=0.43$, $r_M=2.78$, respectively. A comprehensive analysis of the microstructure of C/M copolymers using various 1D (^{1}H, ^{13}C{^{1}H}, DEPT-45, 90, 135) and 2D (HSQC, TOCSY, HMBC) NMR experiments has been done. Unambiguous spectral assignments have been done for the complex and overlapped carbonyl region has been assigned with the aid of 2D HMBC studies. Thermal studies showed that incorporation of higher amounts of MMA into the copolymer lowered the glass transition temperature by rendering flexibility to the polymeric chain.

Acknowledgements

Meghna Markanday thanks the Council of Scientific and Industrial Research, India for financial assistance.

References

[1] Patrickios SC, Krasia T. Polymer 2002;43:2917.
[2] Hwang J, Moon H, Seo J, Park SY, Aoyama T, Wada T, et al. Polymer 2001;42:3023.
[3] Sanda F, Nakai T, Kobayashi N, Masuda T. Macromolecules 2004;37:2703.
[4] Meerholz K, Volodin LB, Sandalphon, Kippelen B, Peyghambarian N. Nature 1994;71:497.
[5] Chang C, Whang W, Hsu C, Lin S. Macromolecules 1999;32:5637.
[6] Hattemer E, Zentel R, Mecher E, Meerholz K. Macromolecules 2000;33:1972.
[7] Shi J, Jiang Z, Cao S. React Funct Polym 2004;59:87.
[8] Ho MS, Barett C, Paterson J, Esteghamatian M, Natansohn A, Rochon P. Macromolecules 1996;29:4613.
[9] Hwang J, Moon H, Seo J, Park SY, Aoyama T, Wada T, et al. Polymer 2001;42:3023.
[10] Chen Y, Zhang B, Wang F. Opt Commun 2003;228:341.
[11] Park SH, Ogino K, Sato H. Synth Met 2000;113:135.
[12] Chen Y, Chen Z, Gong Q, Schroers M. Mater Lett 2003;57:2271.
[13] Kim DW, Moon H, Park SY, Hong II S. React Funct Polym 1999;42:73.
[14] Grazulevicius JV, Strohriegl P, Pielichowski J, Pielichowski K. Prog Polym Sci 2003;28:1297.
[15] Biswas M, Das SK. Polymer 1982;23:1713.
[16] Wang L, Zhang Y, Wada T, Sasabe H. Appl Phys Lett 1996;69:728.
[17] Sanda F, Nakai T, Kobayashi N, Masuda T. Macromolecules 2004;37:2703.
[18] Wang G, Qian S, Xu J, Wang W, Liu X, Li F. Physica Part B 2000;279:116.
[19] Chen Y, He Y, Wang F, Chen H, Gong Q. Polymer 2001;42:1101.
[20] Oshima R, Biswas M, Wada T, Uryu T. J Polym Sci, Polym Lett Ed 1985;23:151.
[21] Chang DM, Gromelski S, Rupp R, Mulvaney JE. J Polym Sci, Chem Ed 1977;15:571.
[22] Burroughes JH, Bradley D, Brown AR, Marks RN, Mackay K, Friend RH, et al. Nature 1990;342:539.
[23] Hu B, Yang Z, Karasz FE. J Appl Phys 1994;76:2419.
[24] Kido J, Shinoya H, Nagai K. Appl Phys Lett 1995;67:2281.
[25] Shui J, Xin Y, Zhang L, Xu S, Cao S. React Funct Polym 2005;62:223.
[26] Brar AS, Kaur M. Polym J 2002;34:325.
[27] Hu CJ, Oshima R, Sato S, Seno M. J Polym Sci, Part C: Polym Lett 1988;26:441.

[28] Uryu T, Ohkawa T, Ohkawa T, Oshima R. Macromolecules 1987;20:712.
[29] Matsuzaki K, Uryu T, Asakura T. NMR spectroscopy and stereoregularity of polymers. Tokyo: Japan Sci. Soc. Press; 1996 [chapter 4].
[30] Kim Y, Harwood HJ. Polymer 2002;43:3229.
[31] Spevacek J, Suchoparek M, Alawi SA. Polymer 1995;36:4125.
[32] Kotyk JJ, Berger PA, Ramson EE. Macromolecules 1990;23:5167.
[33] Dond L, Hill DJT, O'Donell JH, Whittaker AK. Macromolecules 1994; 27:1830.
[34] Hatada K, Kitayama T, Terawaki Y, Sato H, Chujo R, Tanaka Y, et al. Polym J 1995;27:11.
[35] Shimozawa K, Saito M, Chujo R. In: Cheng HN, English AD, editors. NMR spectroscopy of polymers in solution and in the solid state. Japan: ACS Symposium series; 2003. p. 208.
[36] Brar AS, Kaur S. J Polym Sci, Part A: Polym Chem 2005;43:1100.
[37] Brar AS, Saini T. J Polym Sci Part A: Polym Chem 2005;13:2810.
[38] Brar AS, Hooda S, Kumar R. J Polym Sci, Part A: Polym Chem 2003; 41:13.
[39] Bulai A, Jimeno ML, Roman JJ. Macromolecules 1995;28:7363.
[40] Tacx JCJF, Van der Veldon GPM, German AL. J Polym Sci, Part A: Polym Chem 1988;26:1439.
[41] Oh JS, Kinney DR, Wang W, Rinaldi P. Macromolecules 2002;35: 2602.
[42] Monwar M, Oh SJ, Rinaldi P, McCord E, Hutchinson RA, Buback MM, et al. Anal Bioanal Chem 2004;378:1414.
[43] Brar AS, Singh G, Shankar R. J Mol Struct 2004;703:69.
[44] Brar AS, Markanday M, Gandhi S. Ind J Chem 2005;44A:58.
[45] Brar AS, Gandhi S, Markanday M. J Mol Struct 2005;734:35.
[46] Brar AS, Singh G, Shankar R. Eur Polym J 2004;40:2679.
[47] Crone G, Natansohn A. J Polym Sci, Part A: Polym Chem 1992;30:1665.
[48] Karali A, Foudakis GE, Dais P. Macromolecules 2000;33:3180.
[49] Robello D. J Polym Sci, Polym Chem Ed 1990;28:1.
[50] Wang X, Kumar J, Tripathy SK. Macromolecules 1997;30:219.
[51] Ostoverkhova O, He M, Twieg RJ, Moerner WE. Chem Phys 2003; 4:732.